Uncoupled Dark States Can Inherit Polaritonic Properties

Carlos Gonzalez-Ballestero,[1] Johannes Feist,[1] Eduardo Gonzalo Badía,[1]
Esteban Moreno,[1] and Francisco J. Garcia-Vidal[1,2,*]
[1]Departamento de Física Teórica de la Materia Condensada and Condensed Matter Physics Center (IFIMAC), Universidad Autónoma de Madrid, E-28049 Madrid, Spain
[2]Donostia International Physics Center (DIPC), E-20018 Donostia/San Sebastián, Spain
(Received 17 June 2016; revised manuscript received 12 August 2016; published 7 October 2016)

When a collection of quantum emitters interacts with an electromagnetic field, the whole system can enter into the collective strong coupling regime in which hybrid light-matter states, i.e., polaritons can be created. Only a small portion of excitations in the emitters are coupled to the light field, and there are many dark states that, in principle, retain their pure excitonic nature. Here we theoretically demonstrate that these dark states can have a delocalized character, which is inherent to polaritons, despite the fact that they do not have a photonic component. This unexpected behavior only appears when the electromagnetic field displays a discrete spectrum. In this case, when the main loss mechanism in the hybrid system stems from the radiative losses of the light field, dark states are even more efficient than polaritons in transferring excitations across the structure.

DOI: 10.1103/PhysRevLett.117.156402

The ability to create and engineer hybrid light-matter states, i.e., polaritons, can bring together the most advantageous properties of both worlds, such as the high speed and delocalization of photons together with the stability and interacting character of matter excitations [1]. In order to create such hybrid light-matter states, it is usually necessary to reach the so-called collective strong coupling (CSC) between a light field and an ensemble of quantum emitters (QEs). This CSC regime is characterized by the coupling of the electromagnetic field to a set of states in the ensemble (the bright states) forming the polaritons [2]. However, many states of the QEs stay uncoupled to the photons and are thus called dark states. Since its first experimental demonstration with Rydberg atoms [3], CSC has been reached in a variety of systems, ranging from atomic beams to ion Coulomb crystals and organic materials [4–11]. Polaritons display a wide range of basic phenomena such as superfluidity [12], Bose-Einstein condensation [13], or lasing [14]. Besides fundamental prospects, polaritonic systems are also interesting for many applications that cover, among others, future quantum technologies [15–17], both light harvesting [18,19] and transport of energy and charge in organic materials [20–22], and even control of chemical reactions [23].

Despite the great deal of attention received by polaritons, the uncoupled dark states have often been ignored as they are assumed not to benefit from the light-matter coupling. Indeed, these pure matter states are considered only a source of losses for polaritons [24], their potential applications being limited to passive operations such as qubit storage [25]. In this Letter, we challenge this standard view of dark states as passive elements in the CSC regime. We show that, whereas this customary picture of dark states being strongly localized works for photonic structures in which the electromagnetic (EM) spectrum is continuous, dark states display a delocalized character, similar to that exhibited by polaritons, in systems that support a discrete EM spectrum. Moreover, we also demonstrate that if the main loss mechanism resides within the EM modes, dark states can be much better excitation carriers than their polariton counterparts.

In this work we consider a very general light-matter system, where we define a set of photonic modes with energies ω_α and creation operators $a_\alpha^\dagger$. These modes interact with an ensemble of N QEs with energies ϵ_j and spin operators σ_j. According to the dipole approximation, the coupling rate is proportional to both the dipole moment of the QEs and the electric field amplitude, $g_{j\alpha} = -\boldsymbol{\mu}_j \cdot \mathbf{E}_\alpha(\mathbf{r}_j)$. The system is described by an extension of the Jaynes-Cummings Hamiltonian [26] ($\hbar = 1$),

$$H_0 = \sum_j \epsilon_j \sigma_j^\dagger \sigma_j + \sum_{i,j} V_{ij}(\sigma_i^\dagger \sigma_j + \sigma_j^\dagger \sigma_i) + \sum_\alpha \omega_\alpha a_\alpha^\dagger a_\alpha + \sum_{j,\alpha}(g_{j\alpha}\sigma_j^\dagger a_\alpha + g_{j\alpha}^* \sigma_j a_\alpha^\dagger), \quad (1)$$

where in the second term we include the dipole-dipole interaction between the emitters, V_{ij}, which we will consider only to first neighbors in this work. In order to describe the losses in both QEs and light modes, both energies ϵ_j and ω_α contain a non-Hermitian imaginary part [26]. As we are interested in the weak pumping regime, this way of introducing losses is completely equivalent to the Lindblad master equation [27]. Under driving, the full Hamiltonian of the system will be $H = H_0 + V(t)$, where

$V(t)$ describes a weak coherent pump of the first QE in the ensemble,

$$V(t) = \Omega_p \cos(\omega_L t) f(t)(\sigma_1^\dagger + \sigma_1), \tag{2}$$

where the pump strength Ω_p is smaller than any other energy scale in the system. The modulation function $f(t)$ is assumed to vary slowly in time such that the pulse is quasimonochromatic. Notice that the coherent optical excitation as modeled by Eq. (2) is only feasible in open EM cavities, where the QEs are coupled to both the cavity modes and free-space radiation. In this way, QEs can be addressed locally, for instance, by near-field optical probes [28], or by an external QE [29].

For illustrative purposes, we will study two particular EM environments, namely, the plasmon modes supported by an infinite silver nanowire (continuous EM spectrum) and those corresponding to a silver nanoparticle (discrete spectrum), but we stress that our findings are very general. Both metallic structures are described as cylinders of radius $r_0 = 55$ nm lying along the z axis, characterized by a Drude-Lorentz permittivity $\varepsilon_m(\omega)$ [30], and embedded in a dielectric with $\varepsilon_d = 2.4$. The plasmon eigenmodes of the nanowire can be analytically calculated [31], whereas the localized surface plasmon (LSP) modes supported by the nanoparticle have been obtained numerically by using a finite element method software (COMSOL MULTIPHYSICS). In order to comply with the full quantum description in Eq. (1), the calculated plasmon modes have been adequately quantized [30]. As for the QEs surrounding both structures, we choose as an example similar parameters than J-aggregated molecules at room temperature [34–36], namely, dipole moment $|\boldsymbol{\mu}_j| \approx 0.75\ e\,\text{nm}$, and energy $\epsilon_j \equiv \epsilon_0 - i\gamma_0/2$, with frequency and decay rate given by $\epsilon_0 = 1.378$ eV and $\gamma_0 = 1$ meV, respectively. For simplicity, we assume they are homogeneously distributed on a cylindrical layer 35 nm above the metallic surface, with a first neighbor distance of 3 nm, and dipole moments oriented radially.

Let us first analyze the case of an infinitely long nanowire (NW). The dispersion relation of this structure is shown in Fig. 1(a) (red line), along with the corresponding polariton dispersion (blue lines). Note that the system is in the CSC regime, since the energy separation between the two polaritons at the anticrossing point ($k_z \approx 12\ \mu\text{m}^{-1}$), known as Rabi splitting, is much larger than the plasmon losses $\text{Im}(\omega)$, shown in Fig. 1(b). In this case, such losses originate from absorption in the metal, and give rise to a finite plasmonic propagation length, displayed in the green curve in Fig. 1(b).

For the infinite NW system, we emulate the continuum nature of the EM spectrum by imposing periodic boundary conditions over a 30 μm long unit cell, containing $N = 1.88 \times 10^6$ QEs. We choose a finite-duration pump pulse, $f(t) = e^{-(t/\tau)^2}$, where the pump is kept

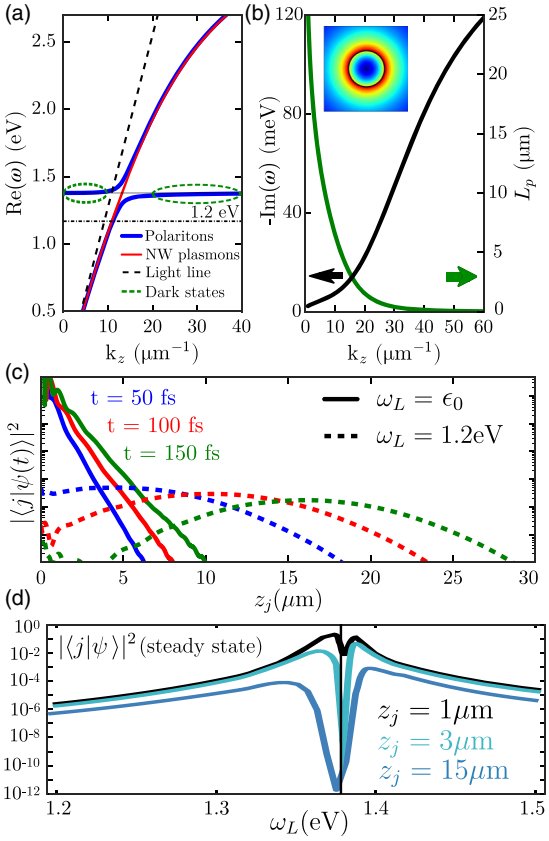

FIG. 1. (a) Plasmon dispersion relation of the infinite nanowire (red) and the corresponding polaritons (blue). (b) Decay rate (black) and propagation length (green) of the plasmons supported by the nanowire. The inset shows the electric field norm of the fundamental mode at 1.4 eV. (c) Population of the QEs as a function of their position, z_j. Solid lines represent the diffusive behavior when pumping the flat region of the band, $\omega_L = \epsilon_0$. Dashed lines show a polariton propagating along the system ($\omega_L = 1.2$ eV). (d) Population in the steady-state versus ω_L, evaluated at three different values of z_j. The vertical line indicates ϵ_0.

quasimonochromatic through a very small frequency window, $\tau^{-1} = 0.01$ eV. Since the pumping rate Ω_p is very weak, the system wave function $|\psi(t)\rangle$ is calculated by standard first-order perturbation theory [30], giving

$$|\psi(t)\rangle = |0\rangle - ie^{-iH_0 t} \int_0^t dt' e^{iH_0 t'} V(t')|0\rangle. \tag{3}$$

The solid lines in Fig. 1(c) show the spatial distribution of the QE population $|\langle j|\psi(t)\rangle|^2 \equiv |\langle 0|\sigma_j|\psi(t)\rangle|^2$, at three different times, when the pump is tuned at the frequency of the dark states, i.e., $\omega_L = \epsilon_0$. In this case, the wave packet is localized at the origin $z = 0$, and the probability spreads along the system in a diffusive manner due to the widening of the initial distribution. Both the strong localization and the diffusive behavior of the wave packet are expected since the pump frequency lies on a flat region

of the dispersion relation, where the group velocity is practically zero, and the associated modes have a purely excitonic, i.e., localized character. Naturally, when the pump frequency lies on a region of nonzero group velocity ($\omega_L = 1.2$ eV), a polariton propagates through the whole nanowire thanks to its photonic component, as visualized by the dashed lines in Fig. 1(c). This distinct spatial behavior between polariton and dark states is also observed in a steady-state situation. For simulating this, a purely monochromatic pulse is chosen, i.e., $f(t) = 1$, which, as a result of the various loss mechanisms, will eventually lead the system into its steady state. In Fig. 1(d), we render the population of the QEs at different positions along the NW, $|\langle j|\psi\rangle|^2$, as a function of the pump frequency ω_L. The three curves show a similar structure in which two maxima, associated with the delocalized polariton modes, are separated by a dip corresponding to the strongly localized dark states.

The spatial extension of dark states, however, is very different when the ensemble of QEs interacts with a *discrete* set of electromagnetic modes. In order to illustrate this, we consider a cylindrical nanoparticle (NP) 300 nm long, terminated by two hemispherical caps as depicted schematically in Fig. 2(a). In the same panel we display the first 9 eigenfrequencies of this structure as a function of mode index n, whereas their corresponding electric field intensities are shown in Fig. 2(b). Note that the second EM mode, $n = 2$, is resonant with the QEs, i.e., $\omega_2 = \epsilon_0$. The number of emitters in this system is $N = 1.88 \times 10^4$, maintaining the same density as in the infinite nanowire case. In a similar manner as in the infinite NW case, we have calculated the steady-state wave function $|\psi\rangle$ both with and without dipole-dipole interaction V_{ij}, in order to have a more complete picture. In the former case, we also account for disorder by performing a statistical average over 10^4 realizations, each of them including a random inhomogeneous broadening in the energy of the QEs, $\epsilon_j \to \epsilon_j + \Delta_j$. The random broadening rate $\Delta_j \in [-\gamma_\phi, \gamma_\phi]$ is bound by the dephasing rate of J-aggregated molecules ($\gamma_\phi \sim 25$ meV) [35].

Let us consider first the case where only the resonant LSP mode ($n = 2$) is included in Eq. (1). For this situation and neglecting dipole-dipole coupling between the QEs, we render in Fig. 3(a) (blue curve) the steady-state population of the QEs lying farthest from the pump region $|\langle N|\psi\rangle|^2$ as a function of the pump frequency ω_L. Notice that similar plots displaying a clear three-peak spectrum are obtained for the populations of every emitter in the ensemble. Therefore, the three maxima in the figure correspond to extended states, where the population is largely delocalized across the system. The two peaks at higher and lower energies are associated with the two polaritons, which inherit the delocalized character of the photonic excitations thanks to their hybrid nature. However, the emergence of a peak located at the frequency of the dark states implies that

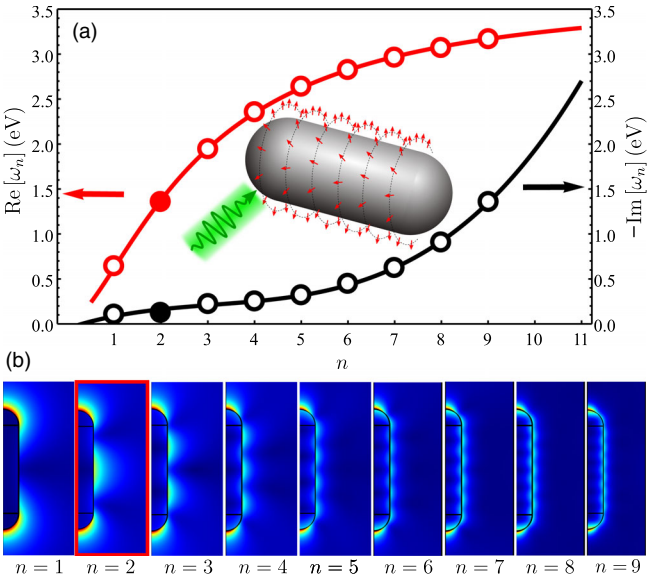

FIG. 2. (a) Numerical results for the real (red) and imaginary parts (black) of the eigenmode frequencies of the metallic nanoparticle. (b) Intensity of the electric field for the corresponding eigenmodes, which are labeled by the mode index n. In our calculations we assume that the $n = 2$ mode is resonant with the excitations in the QEs and this mode is highlighted in both panels.

the population of these modes also extends over the whole system. Notably, this population is several orders of magnitude larger than those of the two polaritons. This is in sharp contrast with the results obtained for an infinite NW. The crossover between these cases, which corresponds to the transition from a discrete to a continuous EM spectrum, happens roughly when the discrete eigenmodes become closely spaced enough to overlap in frequency. A detailed study of this crossover is shown in the Supplemental Material [30].

The peak in the population spectrum related to the dark states remains when both dipole-dipole interaction and disorder are taken into account, as shown by the red curve in Fig. 3(a). No qualitative changes are observed as compared to the previous case, since the tendency to localization introduced by disorder is partially compensated by the dipole-dipole interaction, which induces delocalization. Moreover, the delocalized character also persists when several EM modes supported by the NP are included in the Hamiltonian, as demonstrated in Fig. 3(b). In this case, the additional strongly detuned plasmon modes induce energy shifts on the QEs, leading to a sideband below the energy of the dark states in Fig. 3(b). Although the population spectrum is modified due to the presence of several EM modes in the system, the larger population associated with the dark modes as compared to those of the polaritons is maintained when the full spectrum of the EM environment is taken into account. Figure 3 demonstrates that our main finding, namely, that dark states can inherit the delocalized character of the polaritons,

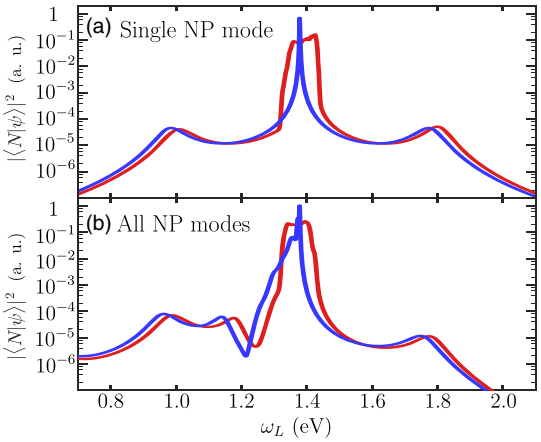

FIG. 3. Steady-state population of the last emitters in the chain, as a function of the pump frequency ω_L. (a) Situation in which only the resonant photonic mode $n = 2$ is taken into account. (b) Same results when including all the modes. Blue lines show the case where dipole-dipole interaction and disorder are neglected, while red lines show the more realistic situation with both included in the Hamiltonian.

is very robust against disorder, dipole-dipole interactions between the QEs, and the existence of several discrete EM modes.

To provide an analytical foundation for our main finding, we now elaborate a simple model that is able to capture the basic ingredients of the interaction of an ensemble of QEs with a photonic structure that displays a discrete EM spectrum. In this model we neglect dipole-dipole coupling and only consider a single EM mode since, as shown in Fig. 3, these two effects play a minor role. We also assume that, as in the numerical calculations presented above, the EM mode is resonant with the excitations within the QEs. In this simple case, the eigenstates of the unperturbed Hamiltonian H_0 are formed by the $(N-1)$ dark states $|D\rangle$, and the upper and lower polariton $|\mathrm{UP}\rangle$ and $|\mathrm{LP}\rangle$, respectively. The former have the same energy as the bare QEs, $\epsilon_j = \epsilon_0 - i\gamma_0/2$. On the other hand, within the CSC regime ($\sqrt{N}g \gg \gamma_0, \gamma_m$), the energies of the states $|\mathrm{UP}\rangle$ and $|\mathrm{LP}\rangle$ are given by $\epsilon_\pm \approx \epsilon_0 - i(\gamma_0+\gamma_m)/4 \pm \sqrt{N}g$, where γ_m is the loss rate of the light mode, and g is the coupling rate of the mode to each of the QEs, which is assumed to be equal for all of them. These eigenstates span the full single-excitation subspace of H_0, i.e.,

$$|\mathrm{UP}\rangle\langle\mathrm{UP}| + |\mathrm{LP}\rangle\langle\mathrm{LP}| + \sum_D |\mathrm{D}\rangle\langle\mathrm{D}| = \mathbb{1}_1. \quad (4)$$

To analyze the dynamics, we start with the general expression for the system wave function $|\psi(t)\rangle$ given in Eq. (3). By introducing the closure relation, Eq. (4), we can calculate the population probability amplitude for a generic emitter j, i.e., $p_j = \langle j|\psi(t)\rangle$, where $|j\rangle \equiv \sigma_j^\dagger|0\rangle$. In the steady state, this magnitude is given by

$$p_j = -\frac{\Omega_p}{2} e^{-i\omega_L t}\left(\frac{\langle j|\mathrm{UP}\rangle\langle\mathrm{UP}|1\rangle}{\epsilon_0-\omega_L+\sqrt{N}g-i(\gamma_0+\gamma_m)/4} + \frac{\langle j|\mathrm{LP}\rangle\langle\mathrm{LP}|1\rangle}{\epsilon_0-\omega_L-\sqrt{N}g-i(\gamma_0+\gamma_m)/4} + \sum_{\mathrm{D}}\frac{\langle j|\mathrm{D}\rangle\langle\mathrm{D}|1\rangle}{\epsilon_0-\omega_L-i\gamma_0/2}\right). \quad (5)$$

According to Eq. (5), the population $|p_j|^2$ will display three well-separated Lorentzian peaks centered at ϵ_0 and $\epsilon_0 \pm \sqrt{N}g$, respectively. Therefore, Eq. (5) is able to account for the numerical results as displayed in Fig. 3(a). It is also straightforward to calculate the ratio between the population peak height associated with the dark modes and those associated with each of the two polaritons; this ratio is proportional to $(1+\gamma_m/\gamma_0)^2$. In the case under study, loss associated with the predominant EM mode of the NP [$\gamma_m \approx 100$ meV, see Fig. 2(a)] is much larger than the loss rate of the QEs ($\gamma_0 \approx 1$ meV). This explains why the population peak of the dark modes in Fig. 3(a) is 4 orders of magnitude higher than the heights of the polariton peaks. It is interesting to note that in the opposite limit, $\gamma_0 \gg \gamma_m$, our analytical formula predicts similar heights for the three population peaks.

Finally, we can also understand the process of dark-state delocalization by first considering $\omega_L \approx \epsilon_0$ and introducing also the closure relation Eq. (4) into Eq. (5), obtaining

$$p_j|_{(\omega_L\approx\epsilon_0)} \propto \frac{\langle j|(\mathbb{1}_1 - |\mathrm{UP}\rangle\langle\mathrm{UP}| - |\mathrm{LP}\rangle\langle\mathrm{LP}|)|1\rangle}{\epsilon_0-\omega_L-i\gamma_0/2}. \quad (6)$$

This expression shows that, in situations in which $\langle j|1\rangle \approx 0$, the dark-state population can be expressed as a function of the two polaritons only. Since both these polaritons are spatially extended, dark states are therefore constrained to display the same delocalized behavior. Note that this is not a property of any particular dark state but of the dark subspace as a whole. In other words, by strongly coupling the QEs to a discrete electromagnetic mode, one extended state is removed from the singly excited Hilbert space. This leaves an imprint on the remaining dark subspace, which hence inherits the delocalized character of the polaritons. This also implies that it is not possible to choose the basis of dark states in such a way that they are completely localized. Note that in principle, Eq. (6) is only valid in the limit of weak disorder and inhomogeneous broadening. However, the numerical results in Fig. 3 demonstrate that dark state delocalization survives even for significant disorder. Importantly, the dark states only acquire the delocalized nature of the polaritons but not their associated losses. As the dark modes do not couple with the EM modes, their losses are only governed by the loss rate of the QEs. When these loss rates are smaller than the radiative losses of the EM modes, dark modes become more efficient in transferring excitations across the system than polaritons.

To conclude, in the collective strong coupling regime of an electromagnetic field to an ensemble of emitters, not only the polaritons but also the dark states can feature a delocalized behavior across the system. This unforeseen result, given the fact that dark states are uncoupled to light, is of a very general nature, requiring only the discrete character of the relevant electromagnetic spectrum. While dark states delocalization is inherited from the corresponding polaritonic behavior, losses are not. This is very advantageous when the population decay is dominated by photon absorption. Thanks to this different perspective on the properties of strongly coupled systems, resonant structures with low to moderate quality factors could thus find a broad range of applications in, among others, excitonic circuits, energy transport, and quantum circuitry.

This work has been funded by the European Research Council (ERC-2011-AdG Proposal No. 290981), the Spanish MECD (FPU13/01225 fellowship), the Spanish MINECO (MAT2014-53432-C5-5-R Grant and the "María de Maeztu" programme for Units of Excellence in R&D (MDM-2014-0377)), and by the European Union Seventh Framework Programme under Grant Agreement No. FP7-PEOPLE-2013-CIG-618229.

*fj.garcia@uam.es

[1] H. J. Kimble, Nature (London) **453**, 1023 (2008).
[2] P. Törmä and W. L. Barnes, Rep. Prog. Phys. **78**, 013901 (2015).
[3] Y. Kaluzny, P. Goy, M. Gross, J. M. Raimond, and S. Haroche, Phys. Rev. Lett. **51**, 1175 (1983).
[4] R. J. Thompson, G. Rempe, and H. J. Kimble, Phys. Rev. Lett. **68**, 1132 (1992).
[5] B. Nagorny, T. Elsässer, and A. Hemmerich, Phys. Rev. Lett. **91**, 153003 (2003).
[6] F. Brennecke, T. Donner, S. Ritter, T. Bourdel, M. Kohl, and T. Esslinger, Nature (London) **450**, 268 (2007).
[7] Y. Colombe, T. Steinmetz, G. Dubois, F. Linke, D. Hunger, and J. Reichel, Nature (London) **450**, 272 (2007).
[8] M. Albert, J. P. Marler, P. F. Herskind, A. Dantan, and M. Drewsen, Phys. Rev. A **85**, 023818 (2012).
[9] D. G. Lidzey, D. D. C. Bradley, M. S. Skolnick, T. Virgili, S. Walker, and D. M. Whittaker, Nature (London) **395**, 53 (1998).
[10] J. Bellessa, C. Bonnand, J. C. Plenet, and J. Mugnier, Phys. Rev. Lett. **93**, 036404 (2004).
[11] J. Dintinger, S. Klein, F. Bustos, W. L. Barnes, and T. W. Ebbesen, Phys. Rev. B **71**, 035424 (2005).
[12] A. Amo, J. Lefrere, S. Pigeon, C. Adrados, C. Ciuti, I. Carusotto, R. Houdre, E. Giacobino, and A. Bramati, Nat. Phys. **5**, 805 (2009).
[13] J. Kasprzak, M. Richard, S. Kundermann, A. Baas, P. Jeambrun, J. M. J. Keeling, F. M. Marchetti, M. H. Szymanska, R. Andre, J. L. Staehli, V. Savona, P. B. Littlewood, B. Deveaud, and L. S. Dang, Nature (London) **443**, 409 (2006).
[14] A. Imamoğlu, R. J. Ram, S. Pau, and Y. Yamamoto, Phys. Rev. A **53**, 4250 (1996).
[15] D. Ballarini, M. De Giorgi, E. Cancellieri, R. Houdré, E. Giacobino, R. Cingolani, A. Bramati, G. Gigli, and D. Sanvitto, Nat. Commun. **4**, 1778 (2014).
[16] A. T. Black, J. K. Thompson, and V. Vuletić, Phys. Rev. Lett. **95**, 133601 (2005).
[17] H. Tanji, S. Ghosh, J. Simon, B. Bloom, and V. Vuletić, Phys. Rev. Lett. **103**, 043601 (2009).
[18] D. M. Coles, Y. Yang, Y. Wang, R. T. Grant, R. A. Taylor, S. K. Saikin, A. Aspuru-Guzik, D. G. Lidzey, J. K.-H. Tang, and J. M. Smith, Nat. Commun. **5**, 5561 (2014).
[19] C. Gonzalez-Ballestero, J. Feist, E. Moreno, and F. J. Garcia-Vidal, Phys. Rev. B **92**, 121402 (2015).
[20] E. Orgiu, J. George, J. Hutchison, E. Devaux, J. Dayen, B. Doudin, F. Stellacci, C. Genet, J. Schachenmayer, C. Genes, G. Pupillo, P. Samorí, and T. Ebbesen, Nat. Mater. **14**, 1123 (2015).
[21] J. Feist and F. J. Garcia-Vidal, Phys. Rev. Lett. **114**, 196402 (2015).
[22] J. Schachenmayer, C. Genes, E. Tignone, and G. Pupillo, Phys. Rev. Lett. **114**, 196403 (2015).
[23] J. A. Hutchison, T. Schwartz, C. Genet, E. Devaux, and T. W. Ebbesen, Angew. Chem., Int. Ed. Engl. **51**, 1592 (2012).
[24] J. del Pino, J. Feist, and F. J. Garcia-Vidal, New J. Phys. **17**, 053040 (2015).
[25] M. Fleischhauer and M. D. Lukin, Phys. Rev. A **65**, 022314 (2002).
[26] H. J. Carmichael, *Statistical Methods in Quantum Optics 2: Non-Classical Fields* (Springer Science & Business Media, Berlin, 2008).
[27] C. Gerry and P. Knight, *Introductory Quantum Optics* (Cambridge University Press, Cambridge, 2005).
[28] T. Taminiau, F. Stefani, F. Segerink, and N. Van Hulst, Nat. Photonics **2**, 234 (2008).
[29] Y. L. A. Rezus, S. G. Walt, R. Lettow, A. Renn, G. Zumofen, S. Götzinger, and V. Sandoghdar, Phys. Rev. Lett. **108**, 093601 (2012).
[30] See Supplemental Material at http://link.aps.org/supplemental/10.1103/PhysRevLett.117.156402 for more details on the calculation of the eigenmodes, quantization of the LSP fields, derivation of analytical expressions for the time-evolved wave function, and study of the transition between discrete and continuum dispersion, which includes Refs. [31–33].
[31] J. D. Jackson, *Classical Electrodynamics* (Wiley, New York, 1999).
[32] Z. M. Wang, *One-Dimensional Nanostructures*, Vol. 3 (Springer Science & Business Media, New York, 2008).
[33] S. A. Maier, *Plasmonics: Fundamentals and Applications* (Springer Science & Business Media, New York, 2007).
[34] J. Moll, S. Daehne, J. R. Durrant, and D. A. Wiersma, J. Chem. Phys. **102**, 6362 (1995).
[35] S. Valleau, S. K. Saikin, M.-H. Yung, and A. A. Guzik, J. Chem. Phys. **137**, 034109 (2012).
[36] T. Schwartz, J. A. Hutchison, J. Léonard, C. Genet, S. Haacke, and T. W. Ebbesen, Chem. Phys. Chem. **14**, 125 (2013).